



IDENTIFICATION OF 200 GeV/c PARTICLES
USING A RING-IMAGING CHERENKOV DETECTOR*

G. Coutrakon, M. Cribier, J. R. Hubbard,
Ph. Mangeot, J. Mullie, and J. Tichit
DPhPE, CEN Saclay, Gif-sur-Yvette, France

and

R. Bouclier, A. Breskin, G. Charpak, J. Million
A. Peisert, J. C. Santiard, and F. Sauli
CERN, Geneva, Switzerland

and

C. N. Brown
Fermi National Accelerator Laboratory
Batavia, Illinois 60510 USA

and

D. Finley, H. Glass, J. Kirz, and R. L. McCarthy
State University of New York at Stony Brook
Stony Brook, New York 11790 USA

November 1981

*Submitted to the IEEE Nuclear Science Symposium, San Francisco,
October 21-23, 1981

large areas, and high data-rate capabilities. We used a narrow-gap proportional wire chamber (PWC) as second stage in the MSAC, and read-out anode and cathode pulses to obtain the three coordinates needed to find the real chamber hits and eliminate ghosts.

We chose helium for the optical medium to limit chromatic dispersion and allow particle identification at high momentum. The helium index of refraction is shown in Fig. 1, along with the quantum efficiency for TEA vapor and the transmission of the CaF_2 crystals used to separate the optical helium from the photoabsorbing chamber gas. Cherenkov angles for π^- , K^- , and p^- are shown in Fig. 2. At 200 GeV/c, π^- and K^- are separated by 0.32 mrad, compared to an RMS chromatic dispersion of 0.06 mrad. Some of our data were taken with methane (CH_4) added to the chamber gas to absorb higher-energy UV photons and reduce the chromatic aberrations.

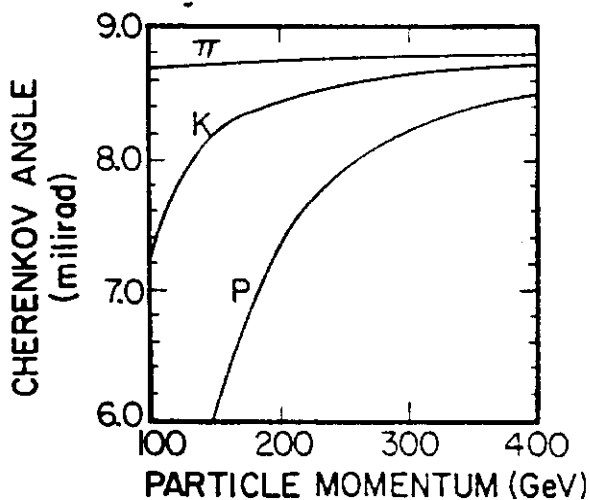


Fig. 2. Cherenkov angle for different momenta and particle types. The refractive index of helium used here was 1.0000386 at STP for 8.6 eV photons.⁶

Experimental Set-up

Figure 3 is a schematic of the apparatus used in the test run at Fermilab. An 8-meter long radiator was placed in an unseparated 200 GeV/c negative hadron beam. Scintillation counters before and after the radiator provided the trigger for reading out the drift chambers and the Cherenkov PWC. Four drift chambers measured the X and Y coordinates of the particle track, before and after the radiator to determine the particle direction. The radiator vessel was a 35-cm diameter stainless-steel tube which had been cleaned and vacuum baked at 100 °C. The radiator was filled with pure helium at atmospheric pressure obtained by boiling liquid helium from a dewar. The gas was warmed to room temperature while flowing through a long copper entrance tube to the radiator. A pure helium

system was necessary because the photon absorption cross sections for oxygen and water are large in our photon energy range. During data taking, a boil-off rate of one liquid liter per hour was used, corresponding to one volume change per hour in the radiator.

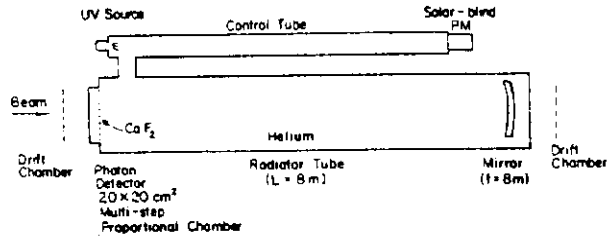


Fig. 3. Experimental set-up.

The helium leaving the radiator passed through a 6-meter long control tube to measure gas transmission. The measurement was made using a UV light source at one end of the tube, and a solar-blind photomultiplier at the other end. The UV source consisted of an Am^{241} alpha source producing UV light in Krypton by dimer emission.⁷ Dimer emission from Krypton is in the energy region that photoionizes TEA. A valve separating the radiator from the control tube could be shut and the control tube evacuated. The ratio of the PM response with and without gas in the tube measured the gas transmission.

The spherical mirror was an 8-inch diameter pyrex substrate vacuum-deposited with an 820 Å layer of aluminum followed by 165 Å of MgF_2 to inhibit oxidation of the aluminum. The reflectivity was measured to be 70% over the entire TEA energy region. The focal length was 794 ± 1.2 cm. Surface roughness before coating was 30 Å RMS, and deviations from perfect sphericity less than 3000 Å.

The 20x20 cm² detector was placed in the upstream end of the tube. An array of four 4-mm thick CaF_2 crystals separated the radiator from the detector and allowed an average transmission of 70% for photons in the TEA energy range. The crystals were mounted on a brass frame to match the CaF_2 thermal expansion. The 1-cm wide arms formed a dead-space for photons, but not for beam tracks.

Photon Detector

The detector structure is shown in Fig. 4. The Cherenkov photons ionize TEA in the conversion gap (C), producing photoelectrons which drift into the preamplification gap (PA). Each photoelectron entering the PA gap initiates an avalanche in the strong electric field. A fraction of the electrons in each avalanche is then transferred through the drift space to the PWC for detection.⁸ The PA gap is needed because the PWC alone has poor single-photon detection efficiency.

A narrow gap was chosen for the PWC to reduce the width of the cathode pulses and improve two-pulse resolution.

The 6 mm conversion gap and the 4 mm PA gap were formed of three stainless-steel meshes of 50 μm -diameter wires, 500 μm apart. The first mesh was in contact with the CaF_2 crystals. The PWC half-gap width was 3.2 mm. Cathode wires were 50 μm -diameter stainless-steel wires spaced every $\frac{1}{2}$ mm. The cathode planes measured X and Y coordinates from induced pulses. Anode wires were 20 μm -diameter copper-beryllium wires at an angle of 45° , spaced every 2 mm. The direct anode pulse provided the U-coordinate, where $U = (X+Y)/2$. All three planes were read-out every 2 mm into analog-to-digital convertors (ADC's).

Results presented here are from two data runs, one with a He(97%)/TEA(3%) gas mixture, and the other with He(87%)/TEA(3%)/CH₄(10%). The mean-free path for photoionization was 0.8 mm in 3% TEA. The drift fields in the conversion and transfer gaps were 100 V/mm for both gas mixtures. With He/TEA the PA gap field was below 600 V/mm, and the PWC

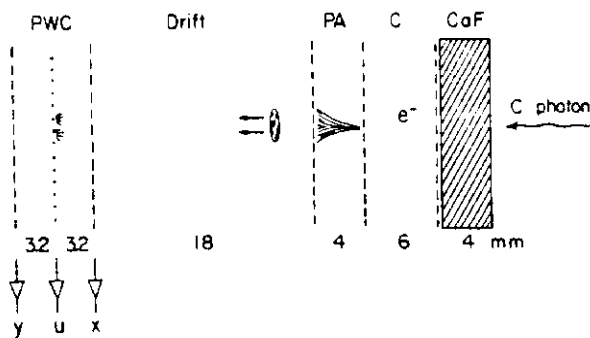


Fig. 4. Photon detector structure.

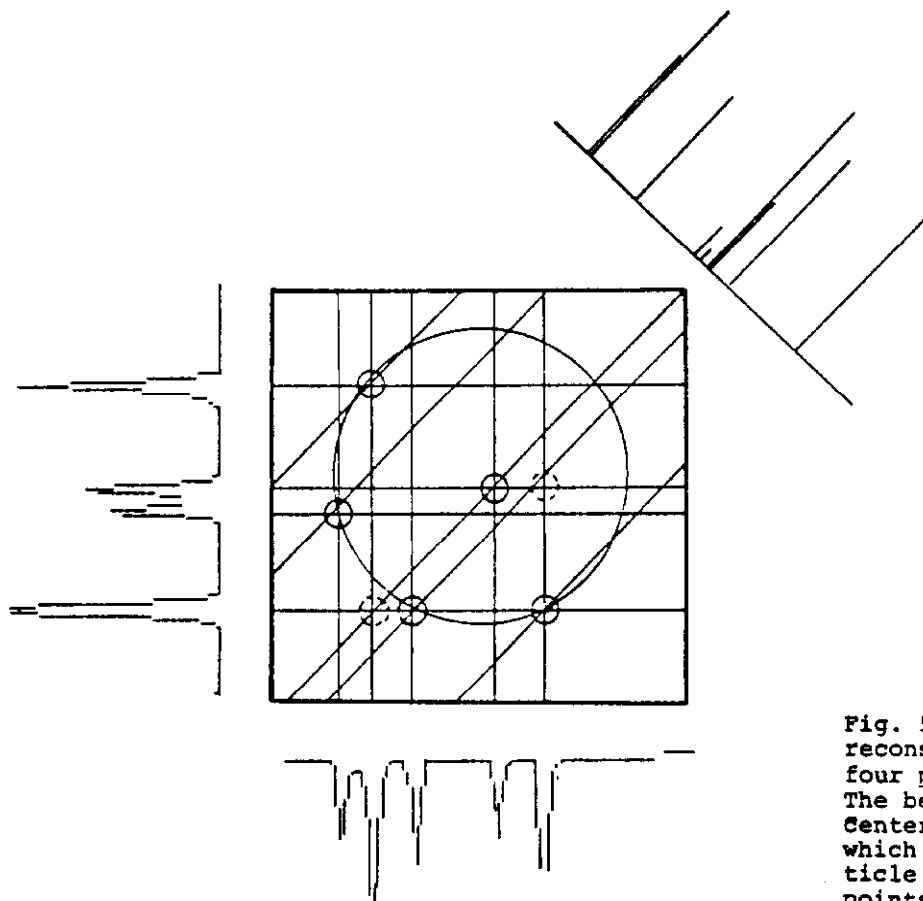


Fig. 5. An example of photon reconstruction for an event with four photons and a beam track. The beam track is not at the center of the Cherenkov ring, which is determined by the particle direction. Two ghost points appear, but they are easily eliminated because all three coordinates are required for other, real points.

anode-cathode voltage difference was 1100 Volts. With He/TEA/CH₄ the PA gap required 1000 V/mm, and the PWC operated at 2000 Volts. We experienced some difficulties with chamber stability, and the higher voltages necessary with He/TEA/CH₄ increased these difficulties.

At the operating voltages, some 10³ charges were transferred to the PWC for each photoelectron entering the PA gap, and the overall gain was about 10⁷. The gain in the PWC was space-charge limited, reducing the amplitude spread in the single-electron pulses.

Data Analysis

Raw data from each event contained ADC pulse-height information from all anode and cathode channels. (Data from a typical event are shown in Fig. 5.) For each photon detected, one or two anode ADC's and typically six ADC's from each cathode plane responded. Coordinates were calculated by the center of gravity method for each group of wires hit. Coordinate triplets (X,Y,U) which were correlated in space to better than the anode wire spacing were accepted as photon candidates if their pulse-height amplitudes were not too different.

Some coordinates were missed or poorly determined because the pulse-height distributions overlapped. To recover these points, we calculated the third coordinate for each coordinate pair, and accepted the candidate point if the contents of the ADC's near the calculated value were sufficient to match the amplitudes of the original pair.

When the candidate search was complete, ghost points were removed and final positions calculated for the accepted points. If two points used a common coordinate, the positions were calculated from the two unique coordinates. If two (or three) of the coordinates of a point were used for more than one point, we attempted to split the measured coordinates and recalculate the center of gravity for the new coordinates by subtracting off the contribution due to previously-resolved points.

Results

The on-line display, summed over 200 events is shown in Fig. 6. (The on-line point-finding routine was simpler than the one described in the previous section.) The width of the ring was mainly due to the spread in the incident particle directions.

On the average, we found 2.7 photons per event in the He/TEA data, and 2.5 per event in the He/TEA/CH₄ data. But fewer events were found with more than four photons than would be expected from a Poisson distribution. In fact, only 5% of the events in the He/Tea run had no photons detected, indicating an average of 3 detectable photons per event. For events with more than one photon, losses occurred because of our limited two-photon resolution and because of pattern-recognition errors. In general, two neighboring photons

were resolved if they were separated by at least 9 mm along the circumference of the Cherenkov ring. This limit resulted from two-coordinate resolving power of 6 mm for the cathodes and 4 mm for the anodes, and a requirement that neighboring photons be resolved in two of three coordinates. About 5% of the photons were unresolved; another 5% were lost by program inefficiencies. Note that the failure to resolve two neighboring photons separated by 9 mm along the ring circumference led to a radius measurement only 150 μ m smaller than the true value.

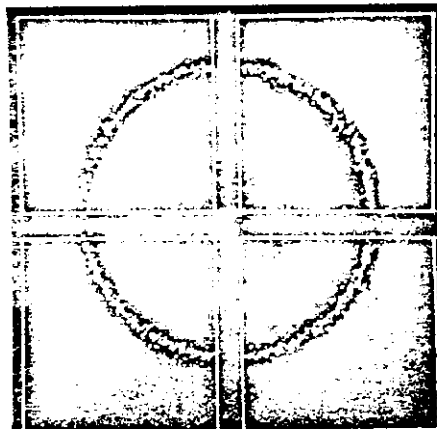


Fig. 6. On-line display summed over 200 events.

The Cherenkov radius calculated from single photons shows a clean peak at the expected π^- radius, with FWHM of 1.7 mm in He/TEA, and 1.3 mm in He/TEA/CH₄. The distributions for He/TEA show a high-radius tail due to the high-energy tail in the TEA quantum efficiency.

The average radius calculated using all photons for each event has a π^- peak with FWHM of 1.2 mm for He/TEA and 0.9 mm for He/TEA/CH₄. The average radius for the He/TEA/CH₄ data are plotted in Fig. 7. The π^- and K^- are at 68.4 and 65.8 mm, respectively, separated by about 6 std. dev.

The average radii distributions are not Gaussian, however, because the single-photon measurement error is not Gaussian, and because the distribution includes events with different numbers of photons.

Better π^-/K^- separation can be obtained on an event-by-event basis by calculating a χ^2 confidence level for each hypothesis ($\pi^-/K^-/p$) with the number of degrees of freedom equal to the number of photons for each event. If the π^- and K^- peaks had equal intensity, we could identify 75% of the events, even in the He/TEA data, with better than 99% confidence. The unidentified events include 5%

with no photons, 5% removed by the present confidence-level cut, and 15% ambiguous between π^- and K^- .

But the quality of the separation depends on the relative intensity of the π^- and K^- signals. In the present data we find 96% π^- , 3.5% K^- and 0.5% antiprotons (at a radius of 57.5 mm). If we weight the confidence levels by the intensities, only K^- are ambiguous within the 5% confidence level. In this case, we identify 90% of the π^- and \bar{p} , but only 70% of the K^- in the He/TEA data.

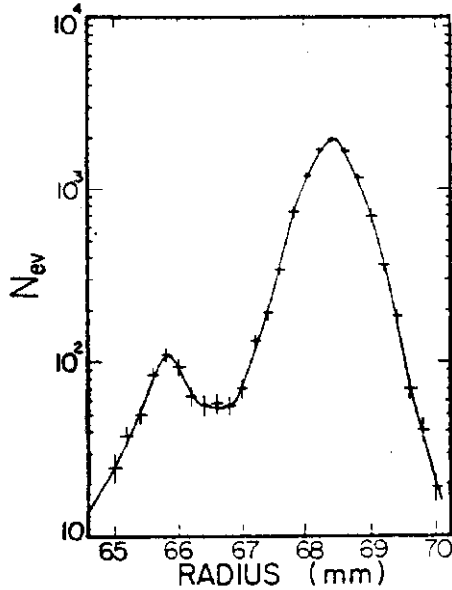


Fig. 7. Distribution of average radii for 10000 events from the He/TEA/CH₄ data run. The curve through the π^- and K^- peaks is hand-drawn.

Future Plans

We are now constructing a 15-meter long Cherenkov counter for the E605 experiment at Fermilab. The device will have a 2.5x2.5 m² aperture and will accept trajectories with divergence ± 60 mrad vertically and ± 30 mrad horizontally. Sixteen mirror elements will focus the Cherenkov photons onto two 40x80 cm² detectors 8-meters from the mirrors, just outside the particle aperture. The detectors have spacers in the PA gap to avoid large gain differences due to electrostatic attraction of the meshes.⁹ This counter will be assembled at Fermilab in February 1982.

References

1. A. Breskin, G. Charpak, S. Majewski, G. Melchart, G. Petersen, and F. Sauli, Nucl. Instr. and Meth. 161 (1979) 19.
2. J. Seguinot and T. Ypsilantis, Nucl. Instr. and Meth. 142 (1977) 377.
3. G. Charpak, S. Majewski, G. Melchart, F. Sauli, and T. Ypsilantis, Nucl. Instr. and Meth. 164 (1979) 419.
4. J. Seguinot, J. Tocqueville, and T. Ypsilantis, Nucl. Instr. and Meth. 173 (1980) 283.
5. G. Comby, Ph. Mangeot, J. L. Augueres, S. Claudet, J. F. Chalot, J. Tichit, H. deLignieres, and A. Zadra, Nucl. Instr. and Meth. 174 (1980) 93.
6. M. C. E. Huber and G. Tondello, J. Opt. Soc. Am. 64 (1974) 390.
7. M. Suzuki and S. Kubota, Nucl. Instr. and Meth. 164 (1979) 197.
8. G. Charpak and F. Sauli, Phys. Lett. 78B (1978) 523.
9. J.R. Hubbard, G. Coutrakon, M. Cribier, Ph. Mangeot, H. Martin, J. Mullie, S. Palanque, and J. Pelle, Nucl. Instr. and Meth. 176 (1980) 233.